Published OnlineFirst May 16, 2014; DOI: 10.1158/1078-0432.CCR-14-0048

Cancer Therapy: Preclinical

Clinical Cancer Research

Gemcitabine and CHK1 Inhibition Potentiate EGFR-Directed Radioimmunotherapy against Pancreatic Ductal Adenocarcinoma

Fares Al-Ejeh[1], Marina Pajic[4,5], Wei Shi[1], Murugan Kalimutho[1], Mariska Miranda[1,3], Adnan M. Nagrial[4], Angela Chou[4,6], Andrew V. Biankin[4,10], Sean M. Grimmond[2,7,10], for the Australian Pancreatic Cancer Genome Initiative, Michael P. Brown[8,9], and Kum Kum Khanna[1,3]

Abstract

Purpose: To develop effective combination therapy against pancreatic ductal adenocarcinoma (PDAC) with a combination of chemotherapy, CHK1 inhibition, and EGFR-targeted radioimmunotherapy.

Experimental Design: Maximum tolerated doses were determined for the combination of gemcitabine, the CHK1 inhibitor PF-477736, and Lutetium-177 (^{177}Lu)–labeled anti-EGFR antibody. This triple combination therapy was investigated using PDAC models from well-established cell lines, recently established patient-derived cell lines, and fresh patient-derived xenografts. Tumors were investigated for the accumulation of ^{177}Lu-anti-EGFR antibody, survival of tumor-initiating cells, induction of DNA damage, cell death, and tumor tissue degeneration.

Results: The combination of gemcitabine and CHK1 inhibitor PF-477736 with ^{177}Lu-anti-EGFR antibody was tolerated in mice. This triplet was effective in established tumors and prevented the recurrence of PDAC in four cell line–derived and one patient-derived xenograft model. This exquisite response was associated with the loss of tumor-initiating cells as measured by flow cytometric analysis and secondary implantation of tumors from treated mice into treatment-naïve mice. Extensive DNA damage, apoptosis, and tumor degeneration were detected in the patient-derived xenograft. Mechanistically, we observed CDC25A stabilization as a result of CHK1 inhibition with consequent inhibition of gemcitabine-induced S-phase arrest as well as a decrease in canonical (ERK1/2 phosphorylation) and noncanonical EGFR signaling (RAD51 degradation) as a result of EGFR inhibition.

Conclusions: Our study developed an effective combination therapy against PDAC that has potential in the treatment of PDAC. *Clin Cancer Res; 20(12); 3187–97. ©2014 AACR.*

Introduction

Pancreatic ductal adenocarcinoma (PDAC) is the fourth most common cause of cancer death, and by 2020, PDAC is anticipated to move to the second leading cause of cancer-related deaths (1). More than 80% of patients with PDAC present with unresectable disease and one third of these patients have locally advanced PDAC; the rest have distant metastases (2). Gemcitabine is a potent radiosensitizing drug and remains the standard of care for locally advanced, unresectable disease (2). Advanced/metastatic PDAC remains one of the most lethal cancers with a median survival of only 6 months. Combinations of gemcitabine and other chemotherapeutics have failed to demonstrate significant clinical benefit with the exception of the recent MPACT and PRODIGE 4/ACCORD 11 randomized controlled trials. MPACT compared gemcitabine and nanoparticle albumin-bound paclitaxel (Abraxane) with gemcitabine alone, and the combination significantly improved overall survival (OS): 8.5 versus 6.7 months (3). PRODIGE 4/ACCORD 11 compared combination FOLFIRINOX (5-fluorouracil, oxaliplatin, irinotecan, and leucovorin) regimen with single-agent gemcitabine, and FOLFIRINOX significantly improved OS (11.1 versus 6.8 months; ref. 4). Despite these incremental benefits, targeted therapies based on

Authors' Affiliations: [1]Signal Transduction Laboratory, QIMR Berghofer Medical Research Institute, Herston; [2]Queensland Centre for Medical Genomics, Institute for Molecular Bioscience, [3]The University of Queensland, St Lucia, Queensland; [4]The Kinghorn Cancer Centre, Cancer Division, Garvan Institute of Medical Research; [5]St Vincent's Clinical School, Faculty of Medicine, University of NSW; [6]Department of Anatomical Pathology, SYDPATH, St Vincent's Hospital, Darlinghurst, New South Wales; [7]Australian Pancreatic Cancer Genome Initiative, for the full list of contributors see http://www.pancreaticcancer.net.au/apgi/collaborators; [8]Cancer Clinical Trials Unit, Royal Adelaide Hospital Cancer Centre, and Centre for Cancer Biology, SA Pathology; [9]School of Medicine, University of Adelaide, Adelaide, Australia; and [10]Wolfson Wohl Cancer Research Centre, Institute of Cancer Sciences, University of Glasgow, Glasgow, Scotland, United Kingdom

Note: Supplementary data for this article are available at Clinical Cancer Research Online (http://clincancerres.aacrjournals.org/).

Corresponding Author: Fares Al-Ejeh, QIMR Berghofer Medical Research Institute, Level 9 Central, 300 Herston Road, Herston, QLD 4006, Australia. Phone: 617-3845-3738; Fax: 617-3362-0105; E-mail: Fares.Al-Ejeh@qimrberghofer.edu.au

doi: 10.1158/1078-0432.CCR-14-0048

Published OnlineFirst May 16, 2014; DOI: 10.1158/1078-0432.CCR-14-0048

Translational Relevance

Pancreatic cancer is a leading cause of cancer-related deaths, and an expected increase in incidence is not matched by an abundance of effective therapies. CHK1 inhibitors in combination with gemcitabine in pancreatic cancer are now entering phase II clinical trials. EGFR inhibition in combination with gemcitabine has been investigated clinically in pancreatic cancer but only produced modest responses. In this study, we describe a novel combination therapy involving gemcitabine and CHK1 inhibitor with radioimmunotherapy tailored specifically to pancreatic ductal adenocarcinomas that express high levels of EGFR. This therapy produced remarkable antitumor responses in several pancreatic cancer models supporting ongoing development of this treatment approach.

the molecular architecture of PDAC offer potential for further survival improvement.

Gemcitabine metabolites, diphosphorylated and triphosphorylated nucleosides (dFdCDP and dFdCTP), cause cell replication stress and activate the checkpoint kinase 1 (CHK1). Preclinical studies investigated the combination of CHK1 inhibitors (CHK1i) with radiotherapy or chemotherapeutics in several cancers, including PDAC. The premise behind this strategy is that the majority of cancer cells are deficient in the G_1–S DNA-damage checkpoint (due to *TP53* mutation). This leads to the reliance of cancer cells on the S and G_2 checkpoint for DNA repair and survival, which can be abrogated using CHK1i (5). Particularly, synthetic lethal RNAi screening identified CHK1 as a sensitizing target for gemcitabine therapy in PDAC (6), and several studies reported the synergistic combination of gemcitabine and CHK1i in animal models (7, 8). The sensitization of pancreatic cancer cell lines by CHK1i correlates with the inhibition of RAD51 (9), which is involved in the homologous recombination (HR) DNA repair pathway. More recently, the combination of CHK1i and gemcitabine together with external local radiotherapy in pancreatic tumor xenografts showed significant delay in tumor growth, which was explained by the abrogation of G_2 checkpoint and inhibition of HR DNA repair (10). Despite the strong antitumor response to this combination therapy, regrowth of tumors was consistently observed (10).

PDAC is a molecularly heterogeneous cancer, with most genomic aberrations occurring at very low frequency (11, 12). Furthermore, recent studies have expounded the intratumoral heterogeneity observed by pathologists for decades. Elaborate clonal evolution radiating from parental clones yields high genetic diversity with a spatial and temporal distribution of cell clones in primary PDAC tumors (13). Although some clones respond to particular treatments, other clones may resist the treatment and drive tumor regrowth. Thus, we rationalized targeting of pancreatic tumor cells using radionuclide-labeled antibody directed against a tumor-associated antigen. Radioimmunotherapy (RIT) overcomes the heterogeneity of tumor cell populations, because radionuclides can kill adjacent antigen-negative tumor cells via a crossfire effect. Moreover, the low dose rate of RIT may alter cell-cycle progression (14), and the G_1 and G_2–M phases of the cell cycle are the most radiosensitive (15).

In this study, we combined gemcitabine and CHK1i with radionuclide therapy delivered using anti-EGFR monoclonal antibody (mAb) to deliver constant radiation dose to pancreatic cancer cells. The rationale was to chemically debulk and radiosensitize tumors using the gemcitabine and CHK1i combination and then to immuno-target radionuclides to antigen-bearing cells, thus delivering radiation crossfire to surrounding antigen-negative cells. Using multiple PDAC xenograft models derived from cell lines and patient tumors, we show that this combination had a profound antitumor effect without any recurrences *in vivo*. This effect was associated with extensive DNA damage, apoptosis, and tumor degeneration and loss of therapy-resistant cell subpopulations.

Materials and Methods

EGFR IHC of PDAC tissue microarrays

A cohort of 104 consecutive patients with primary operable, untreated PDAC who underwent pancreatectomy with curative intent (preoperative clinical stages I and II) was recruited as part of the Australian Pancreatic Cancer Genome Initiative (APGI), and the International Cancer Genome Consortium. Detailed clinicopathologic characteristics of the cohort have been previously described (11). IHC for EGFR was performed as previously described (16; detailed in Supplementary Methods).

Patient-derived xenografts and cell lines generation

The generation of patient-derived xenografts (PDX) and cell lines is detailed in Supplementary Methods. Briefly, female NOD/SCID/IL2 receptor (IL2R) γ (null) (NSG) mice and athymic balb/c-nude mice were used for the establishment of PDXs according to methodology published elsewhere (17). Patient-derived cell lines (PDCL) were established from enzymatically digested xenografts (detailed in Supplementary Methods). None of the PDXs or PDCLs used in this study had mutations in EGFR or HER2, but all were KRAS mutant (data not shown).

Cell culture and anti-EGFR mAb production

The established cell lines PANC-1 (CRL-1469) and BxPC-3 (CRL-1687) were purchased from ATCC and cultured in the recommended ATCC media. PANC-1 and BxPC-3 cells expressing luciferase were prepared by transduction with the luciferase expressing retrovirus as described previously (16). The hybridoma producing the anti-human EGFR mouse mAb (clone 225 HB-8508; IgG1; ATCC) was cultured as per ATCC instructions. This mouse mAb is the

Published OnlineFirst May 16, 2014; DOI: 10.1158/1078-0432.CCR-14-0048

precursor to the derived chimeric human:murine antibody C225, commercially known as cetuximab. The PDCLs TKCC-07 and TKCC-10 were cultured in M199/Ham F12 media mixture (see Supplementary Methods for media description). All the cell lines were regularly tested for mycoplasma and authenticated using short tandem repeat profiling.

The EGFR mAb was purified, conjugated to DOTA-NHS-ESTER (Macrocyclics), radiolabeled with $^{177}LuCl_3$ (Perkin Elmer), and confirmed for immunoreactivity and stability as described elsewhere (16). The specific activity of ^{177}Lu-anti-EGFR mAb ranged between 2 and 3 μCi/μg (74–111 MBq/mg).

Treatments *in vitro* and *in vivo*

Gemcitabine was purchased from Selleck Chemicals LLC, and the CHK1i PF-477736 was provided by Pfizer (compound transfer program grant WS835429). *In vitro* treatments and assays are described in Supplementary Methods.

For *in vivo* therapy experiments, the Animal Ethics Committee of the Queensland Institute of Medical Research gave approval for use of the mice. For cell line–derived models, balb/c nude mice at 5 weeks of age (Animal Resources Centre, ARC) were inoculated subcutaneously with exponentially growing cells (5×10^6 per mouse) prepared in 50 μL of 50:50 PBS:Matrigel (BD Biosciences) solution. For the PDXs, pieces (~4 mm^3) prepared from *in vivo* passage of TKCC-PDX-07 were implanted subcutaneously along with 20 μL of Matrigel. In all models, treatments were initiated when tumors were 60 ± 1 mm^3 as calculated by caliper measurement of tumor's longest (a) and shortest (b) diametersand the equation: tumor volume (mm^3) = $a/2 \times b^2$. Gemcitabine was prepared in saline and administered intravenously on days 1, 4, 7, and 10. The CHK1i PF-477736 was administered subcutaneously at 15 mg/kg as two 7.5 mg/kg injections per day on days 1, 4, 7, and 10. The anti-EGFR mAb was administered intravenously either unlabeled (50 μg per 20 g mouse) or labeled with ^{177}Lu (50 μg with 6 MBq radioactivity per 20 g mouse) injected intravenously on day 2 only. Mouse weights and tumor volumes were measured twice per week in the first 3 weeks of treatment and then once a week.

In vivo and *ex vivo* analyses

For the luciferase-tagged PANC-1 and BxPC-3 models, bioluminescence live imaging (BLI) was carried out using the IVIS100 live animal imaging system (Caliper Life Sciences) at 10 minutes after intraperitoneal injection of 125 mg/kg VivoGlow Luciferin (Promega Corporation). These models were also subjected to BLI to measure the activation of caspase-3 *in vivo* using the VivoGlo caspase-3/7 substrate (Promega Corporation) as described previously (16).

The PDXs TKCC-PDX-07 model was used to perform several *ex vivo* studies. First, to study tumor-initiating cells, tumors were excised at 10 days after treatment start to prepare single-cell suspensions by collagenase B digestion as described previously (16). The single-cell suspensions were used immediately to inoculate new balb/c nude mice (treatment naïve), which were followed for tumor formation (5×10^6 cells in 50 μL of 50:50 PBS:Matrigel). Additional aliquots from the single-cell suspensions were also used for flow cytometric analysis of pancreatic cancer stem cells (CSC) by staining (30 minutes at 4°C) with anti-CD44 PE-Cy5-mAb, anti-CD24 PE-mAb, and anti-EpCAM FITC-mAb (all from BD Biosciences) as per the manufacturer's instructions. Acquisition and analysis were performed using BD FACSCanto II flow cytometer. The PDX model was also used to study the biodistribution of ^{177}Lu-anti-EGFR mAb. Mice were killed at 6 days after the injection of ^{177}Lu-anti-EGFR mAb, and the accumulation of ^{177}Lu was calculated as the percentage of radioactivity counted (Packard Cobra II Gamma Counter; Perkin Elmer) per gram of tissue to the total radioactivity injected. Finally, the TKCC-PDX-07 model was used for histologic and immunoblotting analyses (detailed in Supplementary Methods).

Statistical analysis

Statistical analysis was performed with GraphPad Prism v5.0 (GraphPad Software). The types of tests used are stated in figure legends.

Results

EGFR expression in patients with PDAC

Studies have suggested EGFR as a negative prognostic factor in PDAC (18, 19). The multimodal therapy in this study incorporates EGFR targeting, thus we examined EGFR protein expression in the prospectively accrued APGI cohort of 104 primary operable patients with PDAC. We found that the majority of PDAC cases were positive for EGFR (n = 92; 88.5%) and of these, 48 had high EGFR expression (46.2%, staining intensity 2 and 3). EGFR expression did not correlate with more advanced disease or poorer survival (Fig. 1A) possibly due to the small number of EGFR-negative tumors in this cohort (n = 12; 11.5%). We also examined EGFR expression in our cohort of PDXs generated from the APGI patient samples (n = 37), and found that EGFR protein levels from the patient tumors and the matched PDXs correlated significantly (Cramer V = 0.49, P = 0.001; Fig. 1B and C). Collectively, these results demonstrate that a significant proportion of PDACs express EGFR, providing a potentially attractive therapeutic target.

Gemcitabine and CHK1 inhibition sensitize to EGFR-directed RIT

The multimodal therapy examined in our study involved a gemcitabine and CHK1 inhibition combination to debulk and radiosensitize tumors with subsequent use of radiolabeled anti-EGFR mAb to deliver constant cytotoxic β-radiation at a low dose rate to cells binding the mAb and to surrounding cells via radiation crossfire.

Published OnlineFirst May 16, 2014; DOI: 10.1158/1078-0432.CCR-14-0048

A

BOX1

EGFR IHC staining intensity	0	1	*P* value*	2	*P* value*	3	*P* value*
Number of patients (*n*)	12	44		42		6	
Median disease-free survival (months)	21.1	13.3	0.272	12.1	0.374	12.2	0.151
Median overall survival (months)	27.8	20.2	0.470	18.4	0.343	23.8	0.452

*Log-rank *P* value of median survival between 0 staining and staining indicated i.e. 1, 2 or 3

B

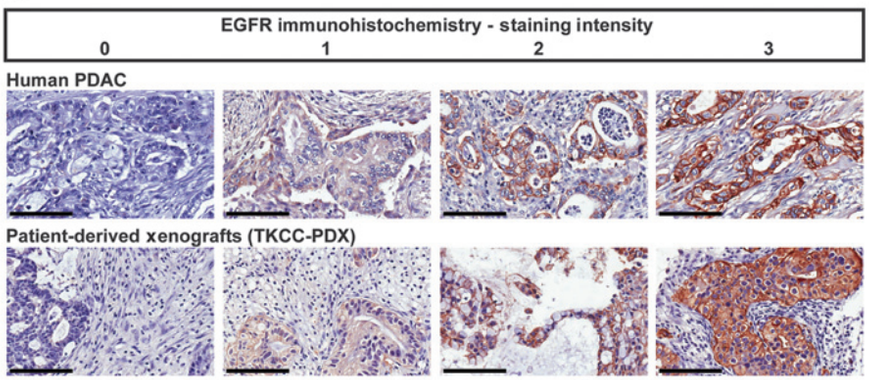

C

BOX2 Observed IHC scores

		Human PDAC TMAs (APGI) Staining intensity				
	PDX TMAs	0	1	2	3	Sums
Staining intensity	0	2	4	2	0	8
	1	0	9	3	0	12
	2	0	1	12	1	14
	3	0	1	1	1	3
	Sums	2	15	18	2	37

Cramer V coefficient of correlation	**0.49061**
P value	**0.00059**

Figure 1. EGFR protein expression in the Australian cohort of PDAC specimens and the patient-derived xenograft model. A, the distribution of EGFR staining intensities among PDAC samples, showing no significant differences in the median disease-free and overall survival between the various subgroups. B, representative images at ×20 magnification showing EGFR protein levels in human PDAC and matched PDXs, with scores corresponding to 0 (absent staining), 1 (incomplete and weak cytoplasmic or incomplete membranous staining), 2 (weak to moderate complete membranous staining), and 3 (strong and complete membranous staining). C, a contingency table showing significant correlation between EGFR protein levels in human PDAC and PDXs ($n = 37$).

First and in line with previous *in vitro* (6) and *in vivo* (7, 8) studies, we confirmed that CHK1 inhibition sensitized the gemcitabine-resistant PANC-1 (20) cell line to gemcitabine treatment. Gemcitabine induced S-phase arrest after 48 hours, and scheduled (16, hours after gemcitabine) or concurrent addition of CHK1i (CHK1i 180 nmol/L; PF-477736; Pfizer) efficiently abrogated this arrest and resulted in apoptotic cell death as judged by the accumulation of cells in subG$_1$ (Supplementary Fig. S1). We subsequently found that CHK1i sensitized the PANC-1 cell line to low continuous radiation dose delivered by targeted RIT using lutetium-177 (^{177}Lu)–labeled anti-EGFR mAb. The clonogenic survival after combining CHK1i (180 nmol/L) with 2 Gy of ^{177}Lu-anti-EGFR mAb (over 72 hours) was similar to that when combining gemcitabine (40 ng/mL) with 2 Gy of ^{177}Lu-anti-EGFR mAb. Importantly, the combination of gemcitabine and CHK1i significantly reduced the clonogenic survival of PANC-1 cells when combined with ^{177}Lu-anti-EGFR mAb (Supplementary Fig. S1).

Tolerability and efficacy of gemcitabine, CHK1i, and EGFR-directed RIT in PDAC models

Our *in vitro* findings indicated that the combination of gemcitabine, CHK1 inhibition, and EGFR-directed RIT as a triple combination therapy could be effective against PDAC. Therefore, we examined the *in vivo* tolerability of the dual and triple combinations. Because we and others (21) have found that concurrent treatment was effective, we administered CHK1i concurrently with gemcitabine instead of a 24-hour delay (7). Dosing schedules of 50 mg/kg gemcitabine and 15 mg/kg (7.5 mg/kg twice daily, b.i.d.) administered every 3 days for 2 cycles with a single dose of ^{177}Lu-anti-EGFR mAb (6 MBq/20 g, 300 MBq/kg) were well tolerated in mice. Higher doses of gemcitabine or EGFR-directed RIT were associated with reversible (>10% weight loss) or irreversible (>30% weight loss) toxicities without an advantage in inhibiting the growth of xenografts (Supplementary Fig. S2). Using the safe doses, we next examined the efficacy of the triple combination of gemcitabine, CHK1 inhibition, and EGFR-directed RIT in xenografts established

Published OnlineFirst May 16, 2014; DOI: 10.1158/1078-0432.CCR-14-0048

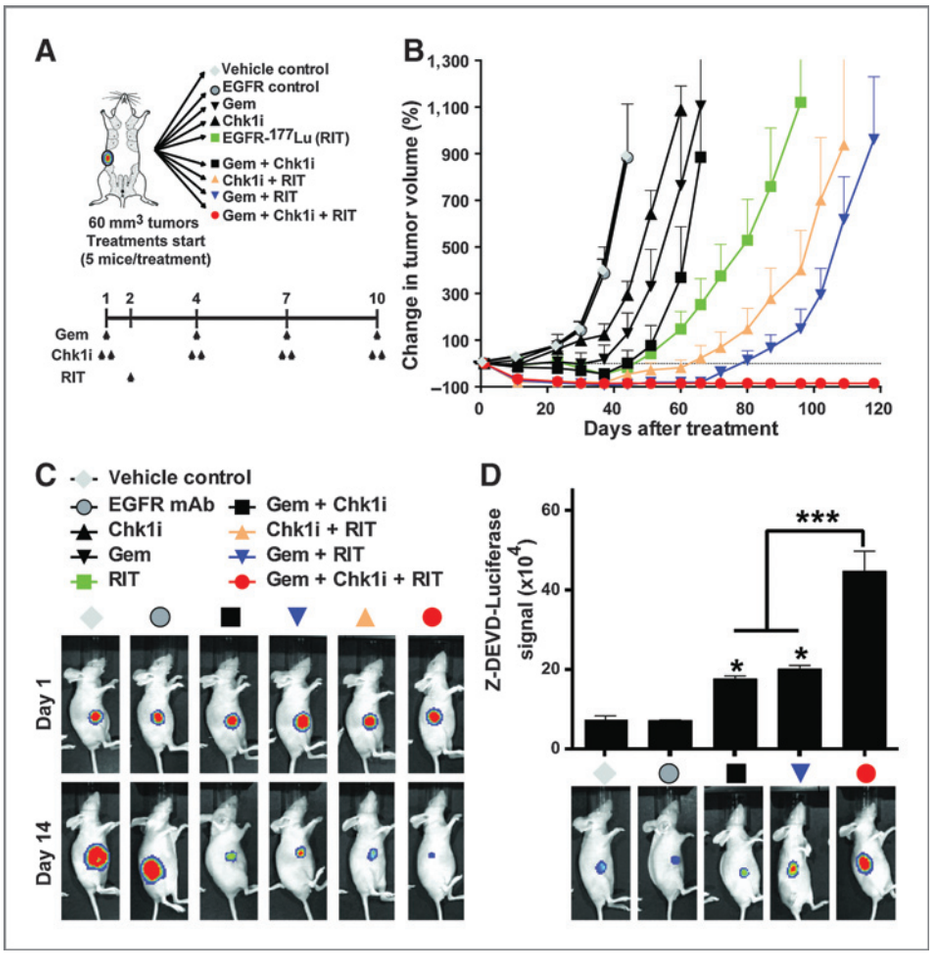

Figure 2. Efficacy of anti-EGFR–directed RIT in combination therapy *in vivo* against PDAC models from ATCC cell lines. Balb/c nude mice bearing the luciferase-expressing PANC-1 and BxPC-3 (Supplementary Fig. S4) xenografts were treated when tumors reached 60 mm^3 in volume. Treatment groups and treatment schedules are outlined in diagram in A. Vehicle control, injection solutions without drugs; EGFR control, intravenous injection of unlabeled anti-EGFR mAb (50 μg per 20 g mouse); CHK1i, two subcutaneous injections per day of the CHK1i PF-477736 at 7.5 mg/kg; Gem, intravenous injection of gemcitabine at 50 mg/kg; RIT, intravenous injection of ^{177}Lu-anti-EGFR mAb (50 μg with 6 MBq radioactivity per 20 g mouse). In combinations, CHK1i was administered 3 hours before and after gemcitabine. B, tumor growth curves presented as the change in tumor volume compared with day 0 (% change +SEM, $n = 5$ mice per treatment group). C, representative images of BLI using Luciferin performed on day 1 (before treatment) and day 14. D, quantification and representative images of BLI using caspase-3/7 substrate (Z-DEVD-Luciferase) performed on day 7 after treatment initiation. Data shown are the average of caspase-3/7 activation (+SEM; $n = 5$ per treatment group). *, $P < 0.05$; ***, $P < 0.001$ in one-way ANOVA in GraphPad Prism.

from two ATCC PDAC cell lines, PANC-1, and BxPC-3. EGFR expression in these cell lines was confirmed by immunoblots and flow cytometry (Supplementary Fig. S3). In comparison with any single- or two-agent combinations, the triple combination therapy produced complete regression of PANC-1 (Fig. 2B and C) and BxPC-3 (Supplementary Fig. S4) tumors. The exquisite response was associated with a remarkable induction of apoptosis as detected by live imaging of caspase-3/7 activation (Fig. 2D and Supplementary Fig. S4). We also observed complete regression of xenografts established from two low-passage (<15) cell lines derived from patients with PDAC, TKCC07 and TKCC10, when treated with the triple combination therapy (Fig. 3A and B).

The efficacy of the triple combination therapy in PDXs

We determined the efficacy of our combination treatment approach in the PDX model (TKCC-PDX-07), which has been generated by direct implantation of patient tumor pieces into immunocompromised mice, and thus has not been subjected to cell culture conditions. All treatment studies were performed in low-passage (third passage) PDXs to limit the potential for clonal selection (17). As shown in Fig. 4A, EGFR-directed RIT alone was as effective as the standard gemcitabine chemotherapy in this model, and gemcitabine or CHK1i potentiated the antitumor effect of RIT. Importantly, complete regression was observed when the triple combination therapy was administered in this PDX model. Moreover, the tumor remnants (day 10

Published OnlineFirst May 16, 2014; DOI: 10.1158/1078-0432.CCR-14-0048

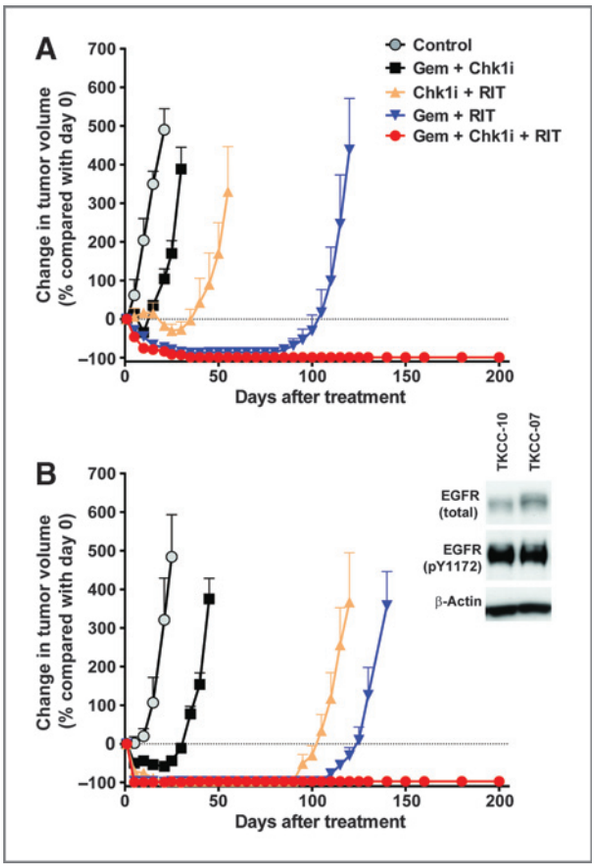

Figure 3. Efficacy of combination treatment *in vivo* against PDAC patient–derived cell lines. Two subcutaneous xenografts (60 mm^3) established from PDAC patient–derived cell lines, TKCC-07 (A) and TKCC-10 (B), were treated as described in Fig. 2. Change in tumor volume was monitored using calipers; data shown are the average change in tumor volume + SEM ($n = 5$ mice per group). Treatment groups are described in A and B, immunoblots of total EGFR protein and phosphorylated EGFR (pY1172) are shown using β-actin as loading control.

after treatment), which completely regressed over time only in the triple combination group, were devoid of tumorigenic cells as judged by the injection of these tumors into new (treatment naïve) mice (Fig. 4B). PDXs treated with the triple combination therapy contained a significantly lower percentage of PDAC tumor-initiating cells identified by flow cytometry as $CD44^+/CD24^+/EpCAM^+$ population (Fig. 4C). We confirmed that the ^{177}Lu-anti-EGFR mAb accumulated in these PDXs at least up to 6 days after injection (Fig. 4D; half-life of ^{177}Lu is 6.7 days), illustrating the continuous delivery of radiation to these tumors.

The triple combination therapy induces DNA damage and tumor tissue degeneration

To determine the mechanism of response, we collected PDXs on day 7 after treatment initiation (6 days after ^{177}Lu-anti-EGFR mAb) for IHC and immunoblotting analyses. We found extensive DNA double-strand breaks (DSB) detected by γH2AX staining and high level of apoptosis detected by ApopTag (TUNEL, terminal deoxynucleotidyl transferase–mediated dUTP nick end labeling) staining following the triple combination treatment (Fig. 5). Consistent with this observation, we detected significant tissue degeneration by both hematoxylin and eosin stain (H&E) and trichrome staining with marked reduction of viable cellular content in relation to collagen (Fig. 5). PDACs are associated with intense collagen fibrotic reactions in the encasing tissue composed of interstitial extracellular matrix and proliferating stromal cells. These collagen reactions contribute to the malignant phenotype of PDAC and the interstitial pressure, which limits the delivery and efficacy of gemcitabine (22, 23) through matrix metalloproteases–dependent ERK1/2 phosphorylation (24). We found that the triple combination therapy significantly reduced collagen in the PDXs (sirius staining in Fig. 5). In comparison with other treatments, the triple combination therapy showed statistically significant increases in DSBs, apoptosis and tissue degeneration, and lower collagen content (Fig. 6A and B). By immunoblotting analysis, we detected CDC25A stabilization in response to CHK1 inhibition. The triple combination therapy reduced the phosphorylation of ERK1/2 and increased degradation of RAD51, which are related to canonical and noncanonical (direct nuclear translocation) pathways of EGFR signaling, respectively (Fig. 6C). Collectively, the results from the PDXs reveal that the inhibition of multiple pathways, including EGFR signaling, DNA damage response, and tumor–stroma interactions, could explain the exquisite efficacy of combining gemcitabine, CHK1 inhibition, and EGFR-directed RIT against PDAC.

Discussion

EGFR is overexpressed at both the mRNA and protein levels in 50% to 60% of PDAC cases (25). High levels of EGFR protein detected by IHC have been associated with faster disease recurrence and shorter survival (18). Although we observed poorer survival in patients with PDAC with EGFR-expressing tumors, it was not statistically significant perhaps because of the low number of its EGFR-negative subgroup and the enrichment of patients with stage I and II PDAC in this cohort. Importantly in our study, EGFR protein is highly expressed in a significant proportion of patients with PDAC patients, presenting a viable therapeutic target.

Therapeutic antibodies against EGFR (cetuximab and matuzumab) and HER2 (trastuzumab) as well as molecular inhibitors (erlotinib, gefitinib, and lapatinib) have been investigated in clinical trials in combination with gemcitabine. These trials failed to demonstrate meaningful clinical benefits in patients with PDAC (26). Failure to demonstrate clinical benefit of targeting other kinases/pathways, such as KRAS, the VEGFR and FGFR amongst others, is a repeated trend in PDAC (26). Similarly, we did not observe any benefit from anti-EGFR mAb as a single agent or in combination with gemcitabine or CHK1i in the PDAC models used in this study. However, a single dose of RIT using ^{177}Lu-labeled anti-EGFR mAb had a similar antitumor effect as gemcitabine. The antitumor effect of EGFR-directed RIT was

Published OnlineFirst May 16, 2014; DOI: 10.1158/1078-0432.CCR-14-0048

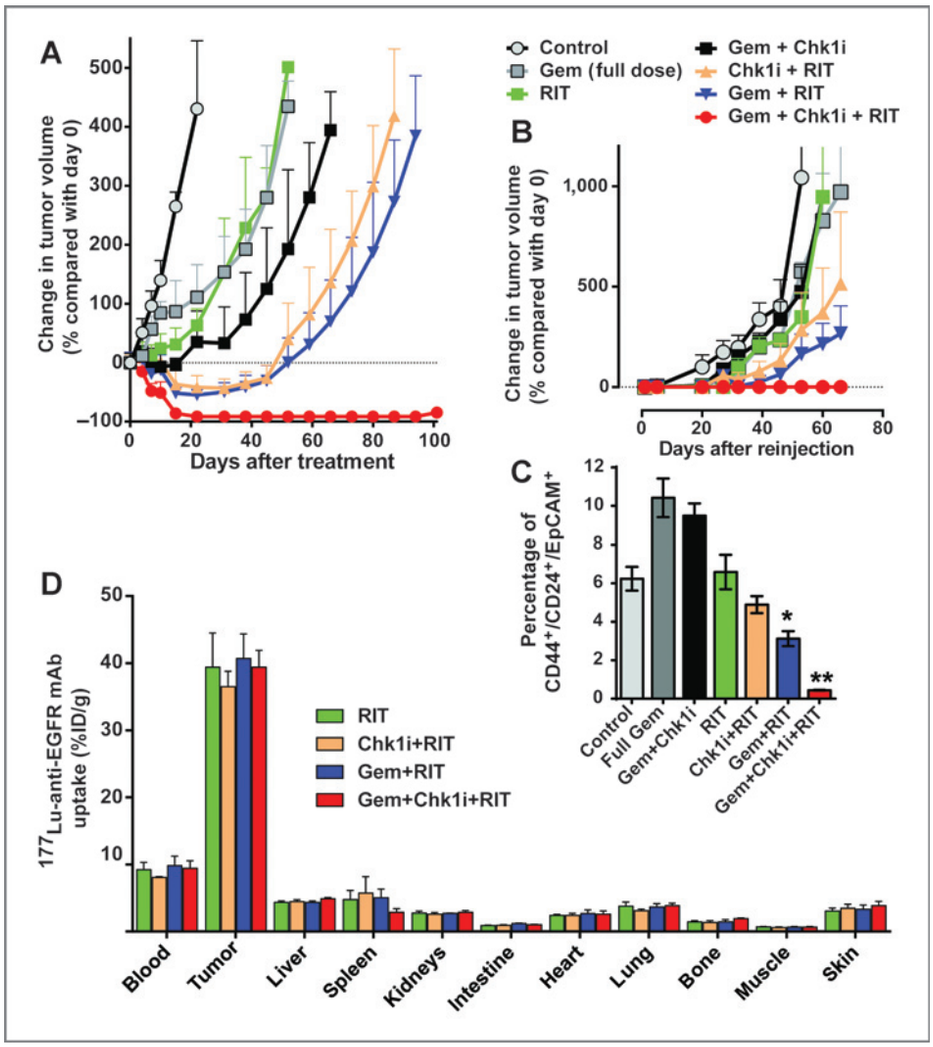

Figure 4. Efficacy of EGFR-directed RIT in combination treatment against PDAC patient–derived xenografts. The PDAC patient–derived xenografts TKCC-PDX-07 (only passaged *in vivo* from patient to mice and never grown as a cell line) were established in balb/c nude mice, and treatments were initiated when tumors reached 50 to 60 mm^3 in volume. Treatments were as described in Fig. 2 with the addition of a new treatment group using the maximum tolerated dose of gemcitabine (Gem Full dose; 150 mg/kg intravenously on days 1, 4, 7, and 10). A, tumor growth curves (average + SEM, $n = 5$). B and C, additional 3 mice per group were treated as described in A and tumors were excised on day 10 to prepare single cell suspensions, which were used immediately to inoculate new mice (B; treatment naïve) and perform FACS analysis of CSCs (C) using CD44, CD24, and EpCAM staining. *, $P < 0.05$; **, $P < 0.01$ compared with control in one-way ANOVA in GraphPad Prism. D, three mice per group were treated as described in A to investigate the biodistribution of the ^{177}Lu-anti-EGFR mAb 6 days after injection.

potentiated by gemcitabine, which indicates radiosensitization as previously reported (27, 28). Importantly, we also found that EGFR-directed RIT was potentiated by CHK1 inhibition. To our knowledge, this is the first study to report that CHK1 inhibition can sensitize cancer cells to the low but constant radiation dose from radionuclides.

Emerging evidence suggests that the capacity of a tumor to grow and propagate depends on a small subset of cells, termed CSCs. Highly tumorigenic pancreatic CSCs have been identified in patient tumors (29, 30). Studies show that gemcitabine resistance correlates with an increased proportion of $CD44^+/CD24^+/EpCAM^+$ and $CD133^+$ cells in pancreatic cancer cell lines (30–32). Clinically, the expression of CD44 and CD133 is associated with poor survival and malignant behavior in patients with pancreatic cancer (32, 33). In agreement, we find that gemcitabine alone or in combination with CHK1 inhibition enriched CSCs in PDAC tumors. However, our findings contradict a previous study reporting a significant reduction of $CD44^+/CD24^+/EpCAM^+$ pancreatic CSCs after gemcitabine alone or combined treatment with the CHK1i AZD7762 and gemcitabine (34). The discordance with our findings could be due to the specificity of the different inhibitors used; AZD7762 has equal potency in inhibiting CHK1 and CHK2 (35), whereas PF-477736 is 100-fold more specific for CHK1 than CHK2 (7). Notably, in contrast to several other reports (30–32), Venkatasubbaiah and colleagues (34) did not report an enrichment of CSCs after gemcitabine treatment. As we have found in PDAC, albeit in a different cancer, lung CSCs were resistant to apoptosis induced by the combination of gemcitabine and the CHK1i PF-477736 in non-CSCs (36). Strikingly, the significant reduction of pancreatic CSCs in our study after triple combination of gemcitabine, CHK1i PF-477736, and EGFR-directed RIT was not only associated with the lack of recurrences in the treated mice, but also the loss of tumorigenicity when the treated tumors were used to inoculate treatment-naïve mice.

CHK1 inhibition using the drugs AZD7762 (10) and MK8776 (37) has been shown to potentiate gemcitabine and external radiotherapy (chemoradiation) due to the

Published OnlineFirst May 16, 2014; DOI: 10.1158/1078-0432.CCR-14-0048

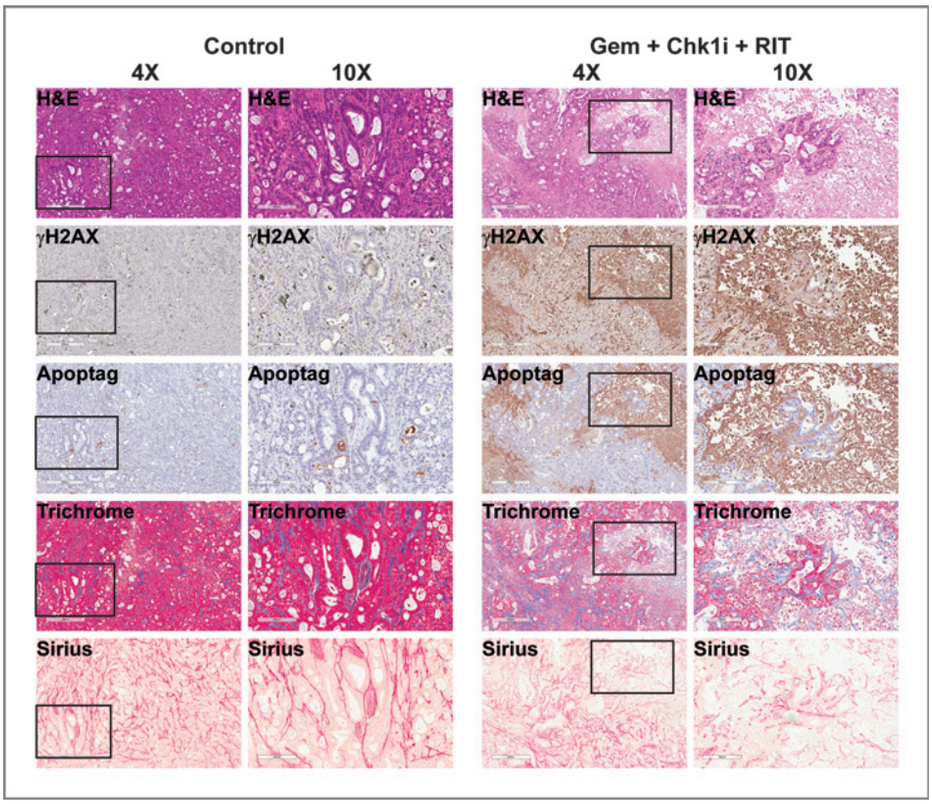

Figure 5. The triple combination therapy causes extensive degeneration of PDAC patient–derived xenografts *in vivo*. Three mice per group bearing the patient-derived xenografts TKCC- PDX-07 were treated as described in Fig. 4, and tumors were collected 7 days after treatment for histologic assessment. Representative images at ×4 and ×10 magnifications are shown from control and triple combination–treated stained with H&E, γH2AX to mark DNA DSBs, ApopTag staining to detect apoptotic cells by the TUNEL method, Masson's Trichrome staining (red for keratin marking cells plasma and blue for collagen fibers and dark red/brown for nuclei) or Sirius red staining specifically for collagen. Boxes in the ×4 magnification images are visualized at ×10 magnification in the adjacent images.

inhibition of the HR DNA repair pathway detected by reduced RAD51 focus formation (9, 10, 37). Here, we also found that CHK1 inhibition augmented the combination of gemcitabine and EGFR-targeted radionuclide therapy. However, in contrast to external beam radiotherapy, which is solely a local treatment, systemic targeted radionuclide therapy has the significant advantage of also treating distant metastases. Another potential benefit of our approach is the choice of target, EGFR, for RIT. EGFR has an emerging role in the maintenance of pancreatic tumor-initiating cells (or CSCs). EGFR is essential for PDAC initiation because its loss in genetically engineered mouse models prevents PDAC development (38–40). Another important feature of EGFR biology that holds clinical promise for RIT is the inhibition of the noncanonical direct EGFR nuclear translocation pathway (41), which increases repair of DNA DSBs (42–45), the most lethal of DNA lesions induced by conventional anticancer treatments. We previously reported that EGFR-directed RIT inhibited DNA-PK phosphorylation, a critical protein involved in nonhomologous end joining pathway of DSBs, and caused the degradation of RAD51, a protein involved in HR repair, in models of aggressive breast cancer (16). In agreement, we report here that EGFR-directed RIT significantly reduced RAD51 in PDAC tumors, and DNA DSBs remained unrepaired as assessed by γH2AX staining. In addition to G_2–M phase arrest with low dose rate of RIT *per se* (14, 46), our results suggest that triple combination therapy exploits multiple and dynamically interacting radiosensitization mechanisms to lower the threshold for apoptosis and achieve therapeutic synergy:

1. Gemcitabine induces dATP pool depletion, CHK1 activation, and S phase arrest (10);
2. CHK1i abrogates the S phase arrest activated by gemcitabine, thus permitting entry of DNA-damaged cells into the radiosensitive G_2–M phase of the cell cycle (15);
3. Anti-EGFR mAb inhibits the activated EGFR in PDAC, and has additional radiosensitizing effect by suppressing DSB repair (HR repair inhibition) via modulation of the noncanonical nuclear EGFR signaling pathway.

Together, these mechanisms may be enough to bypass the overriding effect that mutant KRAS has on the therapeutic blockade of canonical EGFR signaling in pancreatic cancer because the PANC-1 cell line and the PDCLs and PDXs in this study were KRAS mutant, whereas the BxPC-3 is KRAS wild type; however, all responded exquisitely to the triple combination therapy.

The bystander effect of RIT may also be an advantage in treating tumor cells residing in hypoxic regions, which are associated with the acquisition of CSC phenotype in PDAC (47). We argue that the binding of anti-EGFR mAb in nonhypoxic regions is close enough (<80 μm) to the hypoxic areas (48) to be in reach of ^{177}Lu, which has a 2-mm maximum path length in tissue. We found that the uptake of

Published OnlineFirst May 16, 2014; DOI: 10.1158/1078-0432.CCR-14-0048

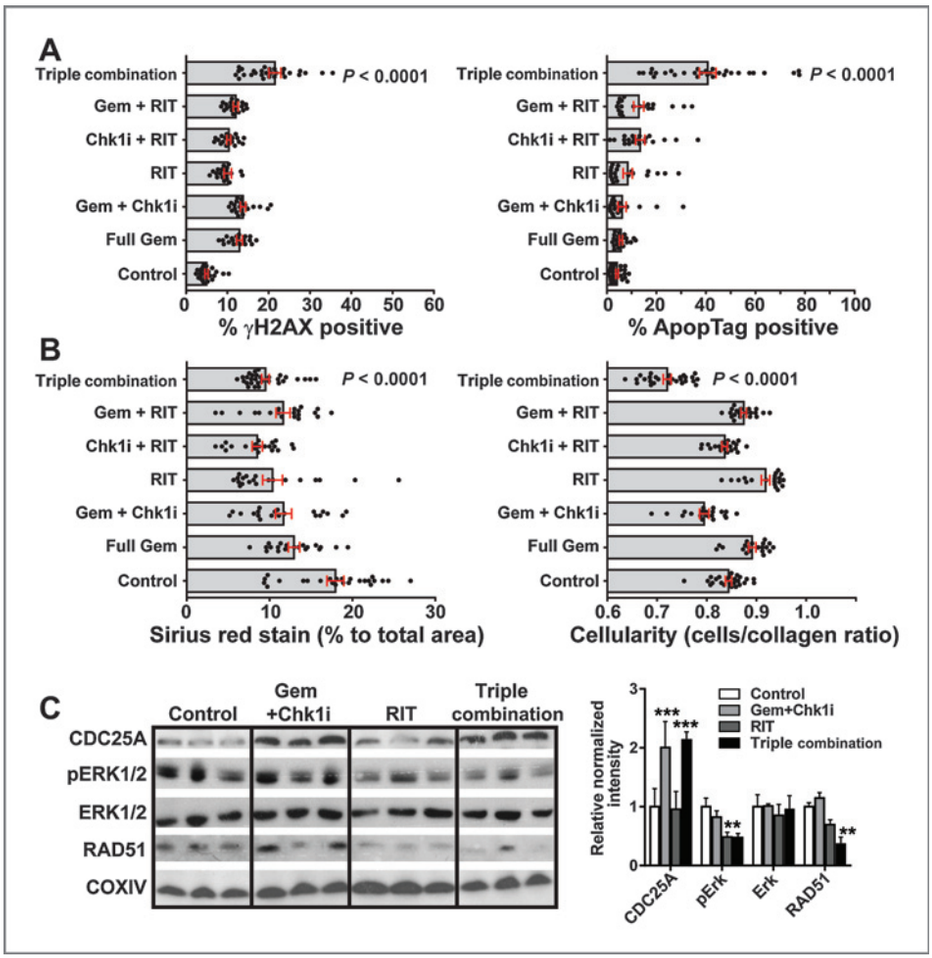

Figure 6. Inhibition of DNA damage repair by the triple combination therapy leads to extensive degeneration of a PDAC PDX. A, quantification of nuclei with phosphorylated H2AX (γH2AX) and ApopTag-stained cells or quantification of collagen staining and cellularity (ratio of red stain for cells to the blue stain for collagen) in the TKCC-PDX-07 (B) at 7 days after therapy. For the quantification in A and B, more than 20 fields at ×10 magnification were obtained from three tumors per treatment group, and positive staining was measured using the ImageJ image analysis software. Bar graphs are the mean (± SEM, $n = 3$) and the scatter dots are the values obtained from all fields analyzed in each treatment group. $P < 0.0001$ for the triple combination compared with control tumors using one-way ANOVA with Bonferroni multiple comparisons test. C, standard immunoblotting was performed using lysates of three tumors from each treatment group prepared at 7 days after therapy. The intensities of bands were quantified, normalized to the loading control (COXIV), and the normalized signal intensities in treated tumors were compared with control tumors. The bar graph shows the normalized signal intensities relative to control tumors ($n = 3$). **, $P < 0.01$; ***, $P < 0.001$ compared with control in two-way ANOVA in GraphPad Prism.

^{177}Lu-anti-EGFR mAb in tumors reached 40% of the injected dose per gram, thus delivering 25 Gy per gram of tumor within the first 6 days. Our *in vivo* studies showed that the triple combination therapy eliminated all xenografts derived from these cell lines despite differences in CSC content of the pancreatic cell lines in our study (data not shown) and the likelihood of tumor hypoxia.

One potential concern about the applicability of EGFR-directed RIT in humans may be liver expression of EGFR (16). However, the lack of clinically evident acute toxicities or impairment in liver and renal functions with anti-EGFR RIT against glioblastoma (49, 50) suggests that this approach may be clinically feasible. Notwithstanding this clinical evidence and our demonstration of high and tumor-specific uptake of the same murine anti-human EGFR clone 225 mAb in a murine breast cancer xenograft model (16), formal toxicologic studies of this new triple combination therapy will be required before the approach can be applied clinically.

In this study, we provide preclinical proof-of-concept for the efficacy of our strategy using optimized doses of each agent, which produce transient loss of no more than 10% of the starting body weight. Nonetheless, these safety data obtained in human xenograft models using the anti-EGFR clone 225 mAb cannot represent an adequate toxicologic assessment of the triple combination therapy because neither clone 225 mAb nor its derivative cetuximab (nor panitumumab) bind murine EGFR in potential target organs such as skin, gut, and liver. Therefore, our future directions in the clinical development of the triple combination therapy will include toxicologic assessments using a mouse anti-mouse EGFR mAb in genetically engineered

Published OnlineFirst May 16, 2014; DOI: 10.1158/1078-0432.CCR-14-0048

murine PDAC models, comparisons of EGFR-directed RIT with other antigen-specific RIT targets such as CEA or MUC1 to determine whether the RIT depends on the unique role that EGFR plays in the maintenance of PDAC tumor-initiating cells, and the investigation of antibodies against active EGFR such as ABT-806 to minimize off-organ, on-target toxicity.

Disclosure of Potential Conflicts of Interest

No potential conflicts of interest were disclosed.

Authors' Contributions

Conception and design: F. Al-Ejeh, M. Kalimutho, A.V. Biankin, M.P. Brown, K.K. Khanna

Development of methodology: F. Al-Ejeh, M. Pajic, M. Miranda, A. Chou, A.V. Biankin, M.P. Brown

Acquisition of data (provided animals, acquired and managed patients, provided facilities, etc.): F. Al-Ejeh, M. Pajic, W. Shi, M. Kalimutho, M. Miranda, A.M Nagrial, A. Chou, S.M. Grimmond

Analysis and interpretation of data (e.g., statistical analysis, biostatistics, computational analysis): F. Al-Ejeh, M. Pajic, W. Shi, A.M Nagrial, A. Chou, A.V. Biankin, M.P. Brown, K.K. Khanna

Writing, review, and or revision of the manuscript: F. Al-Ejeh, M. Pajic, W. Shi, M. Miranda, A.M Nagrial, A. Chou, A.V. Biankin, M.P. Brown, K.K. Khanna

Administrative, technical, or material support (i.e., reporting or organizing data, constructing databases): F. Al-Ejeh, A.V. Biankin, K.K. Khanna

Study supervision: F. Al-Ejeh, K.K. Khanna

Grant Support

This work was supported by the Cancer Council New South Wales Innovator Grant (IG09-04 to F. Al-Ejeh), the Justin McDonald Pancreatic Cancer grant (to F. Al-Ejeh), Australian Research Council (ARC) Future Fellowship (FT130101417 to F. Al-Ejeh), and the National Health and Medical Research Council (NHMRC) Program Grant (to K.K. Khanna).

The costs of publication of this article were defrayed in part by the payment of page charges. This article must therefore be hereby marked *advertisement* in accordance with 18 U.S.C. Section 1734 solely to indicate this fact.

Received January 8, 2014; revised March 17, 2014; accepted April 1, 2014; published OnlineFirst May 16, 2014.

References

1. Matrisian LM, Aizenberg R, Rosenzweig A. The alarming rise of pancreatic cancer deaths in the United States: why we need to stem the tide today [monograph on the Internet]; 2012 [cited 2013 Jan 23]. Available from: http://www.pancan.org/wp-content/uploads/2013/01/incidence_report_2012.pdf published by the Pancreatic Cancer Action Network (Manhattan Beach, CA, USA).
2. Brunner TB, Scott-Brown M. The role of radiotherapy in multimodal treatment of pancreatic carcinoma. Radiat Oncol 2010;5:64.
3. Von Hoff DD, Ervin T, Arena FP, Chiorean EG, Infante J, Moore M, et al. Increased survival in pancreatic cancer with nab-paclitaxel plus gemcitabine. N Engl J Med 2013;369:1691–703.
4. Conroy T, Desseigne F, Ychou M, Bouche O, Guimbaud R, Becouarn Y, et al. FOLFIRINOX versus gemcitabine for metastatic pancreatic cancer. N Engl J Med 2011;364:1817–25.
5. Al-Ejeh F, Kumar R, Wiegmans A, Lakhani SR, Brown MP, Khanna KK. Harnessing the complexity of DNA-damage response pathways to improve cancer treatment outcomes. Oncogene 2010;29:6085–98.
6. Azorsa DO, Gonzales IM, Basu GD, Choudhary A, Arora S, Bisanz KM, et al. Synthetic lethal RNAi screening identifies sensitizing targets for gemcitabine therapy in pancreatic cancer. J Transl Med 2009;7:43.
7. Blasina A, Hallin J, Chen E, Arango ME, Kraynov E, Register J, et al. Breaching the DNA damage checkpoint via PF-00477736, a novel small-molecule inhibitor of checkpoint kinase 1. Mol Cancer Ther 2008;7:2394–404.
8. Matthews DJ, Yakes FM, Chen J, Tadano M, Bornheim L, Clary DO, et al. Pharmacological abrogation of S-phase checkpoint enhances the anti-tumor activity of gemcitabine in vivo. Cell cycle 2007;6:104–10.
9. Parsels LA, Morgan MA, Tanska DM, Parsels JD, Palmer BD, Booth RJ, et al. Gemcitabine sensitization by checkpoint kinase 1 inhibition correlates with inhibition of a Rad51 DNA damage response in pancreatic cancer cells. Mol Cancer Thera 2009;8:45–54.
10. Morgan MA, Parsels LA, Zhao L, Parsels JD, Davis MA, Hassan MC, et al. Mechanism of radiosensitization by the Chk1/2 inhibitor AZD7762 involves abrogation of the G2 checkpoint and inhibition of homologous recombinational DNA repair. Cancer Res 2010;70:4972–81.
11. Biankin AV, Waddell N, Kassahn KS, Gingras MC, Muthuswamy LB, Johns AL, et al. Pancreatic cancer genomes reveal aberrations in axon guidance pathway genes. Nature 2012;491:399–405.
12. Jones S, Zhang X, Parsons DW, Lin JC, Leary RJ, Angenendt P, et al. Core signaling pathways in human pancreatic cancers revealed by global genomic analyses. Science (New York, NY 2008;321:1801–6.
13. Yachida S, Jones S, Bozic I, Antal T, Leary R, Fu B, et al. Distant metastasis occurs late during the genetic evolution of pancreatic cancer. Nature 2010;467:1114–7.
14. Langmuir VK, Fowler JF, Knox SJ, Wessels BW, Sutherland RM, Wong JY. Radiobiology of radiolabeled antibody therapy as applied to tumor dosimetry. Med Phys 1993;20:601–10.
15. Al-Ejeh F, Brown MP. Combined modality therapy: relevance for targeted radionuclide therapy In:Speer TW, editor. Targeted radionuclide therapy. Philadelphia: Lippincott Williams & Wilkins; 2010. p. 220–35.
16. Al-Ejeh F, Shi W, Miranda M, Simpson PT, Vargas AC, Song S, et al. Treatment of triple-negative breast cancer using anti-EGFR-directed radioimmunotherapy combined with radiosensitizing chemotherapy and PARP inhibitor. J Nucl Med 2013;54:913–21.
17. Rubio-Viqueira B, Jimeno A, Cusatis G, Zhang X, Iacobuzio-Donahue C, Karikari C, et al. An in vivo platform for translational drug development in pancreatic cancer. Clin Cancer Res 2006;12:4652–61.
18. Yamanaka Y, Friess H, Kobrin MS, Buchler M, Beger HG, Korc M. Coexpression of epidermal growth factor receptor and ligands in human pancreatic cancer is associated with enhanced tumor aggressiveness. Anticancer Res 1993;13:565–9.
19. Ueda S, Ogata S, Tsuda H, Kawarabayashi N, Kimura M, Sugiura Y, et al. The correlation between cytoplasmic overexpression of epidermal growth factor receptor and tumor aggressiveness: poor prognosis in patients with pancreatic ductal adenocarcinoma. Pancreas 2004;29:e1–8.
20. Akada M, Crnogorac-Jurcevic T, Lattimore S, Mahon P, Lopes R, Sunamura M, et al. Intrinsic chemoresistance to gemcitabine is associated with decreased expression of BNIP3 in pancreatic cancer. Clin Cancer Res 2005;11:3094–101.
21. Zhang C, Yan Z, Painter CL, Zhang Q, Chen E, Arango ME, et al. PF-00477736 mediates checkpoint kinase 1 signaling pathway and potentiates docetaxel-induced efficacy in xenografts. Clin Cancer Res 2009;15:4630–40.
22. Olive KP, Jacobetz MA, Davidson CJ, Gopinathan A, McIntyre D, Honess D, et al. Inhibition of Hedgehog signaling enhances delivery of chemotherapy in a mouse model of pancreatic cancer. Science 2009;324:1457–61.
23. Armstrong T, Packham G, Murphy LB, Bateman AC, Conti JA, Fine DR, et al. Type I collagen promotes the malignant phenotype of pancreatic ductal adenocarcinoma. Clin Cancer Res 2004;10:7427–37.
24. Dangi-Garimella S, Krantz SB, Barron MR, Shields MA, Heiferman MJ, Grippo PJ, et al. Three-dimensional collagen I promotes gemcitabine resistance in pancreatic cancer through MT1-MMP-mediated expression of HMGA2. Cancer Res 2011;71:1019–28.
25. Korc M, Chandrasekar B, Yamanaka Y, Friess H, Buchier M, Beger HG. Overexpression of the epidermal growth factor receptor in human pancreatic cancer is associated with concomitant increases in the

Published OnlineFirst May 16, 2014; DOI: 10.1158/1078-0432.CCR-14-0048

levels of epidermal growth factor and transforming growth factor alpha. J Clin Invest 1992;90:1352–60.
26. Preis M, Korc M. Kinase signaling pathways as targets for intervention in pancreatic cancer. Cancer Biol Ther 2010;9:754–63.
27. Gold DV, Modrak DE, Schutsky K, Cardillo TM. Combined 90Yttrium-DOTA-labeled PAM4 antibody radioimmunotherapy and gemcitabine radiosensitization for the treatment of a human pancreatic cancer xenograft. Int J Cancer 2004;109:618–26.
28. Al-Ejeh F, Darby JM, Brown MP. Chemotherapy synergizes with radioimmunotherapy targeting La autoantigen in tumors. PLoS ONE 2009;4:e4630–e42.
29. Li C, Heidt DG, Dalerba P, Burant CF, Zhang L, Adsay V, et al. Identification of pancreatic cancer stem cells. Cancer Res 2007;67:1030–7.
30. Hermann PC, Huber SL, Herrler T, Aicher A, Ellwart JW, Guba M, et al. Distinct populations of cancer stem cells determine tumor growth and metastatic activity in human pancreatic cancer. Cell Stem Cell 2007;1:313–23.
31. Shah AN, Summy JM, Zhang J, Park SI, Parikh NU, Gallick GE. Development and characterization of gemcitabine-resistant pancreatic tumor cells. Ann Surg Oncol 2007;14:3629–37.
32. Hong SP, Wen J, Bang S, Park S, Song SY. CD44-positive cells are responsible for gemcitabine resistance in pancreatic cancer cells. Int J Cancer 2009;125:2323–31.
33. Maeda S, Qiang D, Shinchi H, Kurahara H, Mataki Y, Maemura K, et al. CD44 and CD133 expressions in primary tumor cells correlate to survival of pancreatic cancer patients. Open Surg Oncol J 2009;1:1–7.
34. Venkatesha VA, Parsels LA, Parsels JD, Zhao L, Zabludoff SD, Simeone DM, et al. Sensitization of pancreatic cancer stem cells to gemcitabine by Chk1 inhibition. Neoplasia 2012;14:519–25.
35. Zabludoff SD, Deng C, Grondine MR, Sheehy AM, Ashwell S, Caleb BL, et al. AZD7762, a novel checkpoint kinase inhibitor, drives checkpoint abrogation and potentiates DNA-targeted therapies. Mol Cancer Ther 2008;7:2955–66.
36. Fang DD, Cao J, Jani JP, Tsaparikos K, Blasina A, Kornmann J, et al. Combined gemcitabine and CHK1 inhibitor treatment induces apoptosis resistance in cancer stem cell-like cells enriched with tumor spheroids from a non-small cell lung cancer cell line. Front Med 2013;7:462–76.
37. Engelke CG, Parsels LA, Qian Y, Zhang Q, Karnak D, Robertson JR, et al. Sensitization of pancreatic cancer to chemoradiation by the Chk1 inhibitor MK8776. Clin Cancer Res 2013;19:4412–21.
38. Ardito CM, Gruner BM, Takeuchi KK, Lubeseder-Martellato C, Teichmann N, Mazur PK, et al. EGF receptor is required for KRAS-induced pancreatic tumorigenesis. Cancer Cell 2012;22:304–17.
39. Navas C, Hernandez-Porras I, Schuhmacher AJ, Sibilia M, Guerra C, Barbacid M. EGF receptor signaling is essential for k-ras oncogene-driven pancreatic ductal adenocarcinoma. Cancer Cell 2012;22:318–30.
40. Eberl M, Klingler S, Mangelberger D, Loipetzberger A, Damhofer H, Zoidl K, et al. Hedgehog-EGFR cooperation response genes determine the oncogenic phenotype of basal cell carcinoma and tumour-initiating pancreatic cancer cells. EMBO Mol Med 2012;4:218–33.
41. Brand TM, Iida M, Li C, Wheeler DL. The nuclear epidermal growth factor receptor signaling network and its role in cancer. Discov Med 2011;12:419–32.
42. Dittmann K, Mayer C, Rodemann HP. Inhibition of radiation-induced EGFR nuclear import by C225 (Cetuximab) suppresses DNA-PK activity. Radiother Oncol 2005;76:157–61.
43. Friedmann BJ, Caplin M, Savic B, Shah T, Lord CJ, Ashworth A, et al. Interaction of the epidermal growth factor receptor and the DNA-dependent protein kinase pathway following gefitinib treatment. Mol Cancer Ther 2006;5:209–18.
44. Ko JC, Ciou SC, Cheng CM, Wang LH, Hong JH, Jheng MY, et al. Involvement of Rad51 in cytotoxicity induced by epidermal growth factor receptor inhibitor (gefitinib, IressaR) and chemotherapeutic agents in human lung cancer cells. Carcinogenesis 2008;29:1448–58.
45. Li L, Wang H, Yang ES, Arteaga CL, Xia F. Erlotinib attenuates homologous recombinational repair of chromosomal breaks in human breast cancer cells. Cancer Res 2008;68:9141–6.
46. Knox SJ, Sutherland W, Goris ML. Correlation of tumor sensitivity to low-dose-rate irradiation with G2/M-phase block and other radiobiological parameters. Radiat Res 1993;135:24–31.
47. Hashimoto O, Shimizu K, Semba S, Chiba S, Ku Y, Yokozaki H, et al. Hypoxia induces tumor aggressiveness and the expansion of CD133-positive cells in a hypoxia-inducible factor-1alpha-dependent manner in pancreatic cancer cells. Pathobiology 2011;78:181–92.
48. Lee CM, Tannock IF. The distribution of the therapeutic monoclonal antibodies cetuximab and trastuzumab within solid tumors. BMC Cancer 2010;10:255.
49. Kalofonos HP, Pawlikowska TR, Hemingway A, Courtenay-Luck N, Dhokia B, Snook D, et al. Antibody guided diagnosis and therapy of brain gliomas using radiolabeled monoclonal antibodies against epidermal growth factor receptor and placental alkaline phosphatase. J Nucl Med 1989;30:1636–45.
50. Li L, Quang TS, Gracely EJ, Kim JH, Emrich JG, Yaeger TE, et al. A Phase II study of anti-epidermal growth factor receptor radioimmunotherapy in the treatment of glioblastoma multiforme. J Neurosurg 2010;113:192–8.

Published OnlineFirst May 16, 2014; DOI: 10.1158/1078-0432.CCR-14-0048

Clinical Cancer Research

Gemcitabine and CHK1 Inhibition Potentiate EGFR-Directed Radioimmunotherapy against Pancreatic Ductal Adenocarcinoma

Fares Al-Ejeh, Marina Pajic, Wei Shi, et al.

Clin Cancer Res 2014;20:3187-3197. Published OnlineFirst May 16, 2014.